Oxide synthesis

https://doi.org/10.1038/s41563-026-02788-z

Writing monolayer oxides with electrons

Ali Zavabeti

Check for updates

Layered metal oxyhalides can be selectively dehalogenated inside a scanning transmission electron microscope, yielding free-standing monolayer oxide sheets and coupling synthesis with atomic-resolution observation.

Reducing metal oxides to a single atomic layer promises electronic, magnetic and catalytic behaviour distinct from that of their bulk counterparts. Most oxides, however, lack the weakly bonded planes that facilitate the exfoliation of graphene-like materials, rendering free-standing sheets at the atomic limit rarely attainable. Now, writing in *Nature Materials*, Meng Gao and co-workers report the use of the imaging probe in scanning transmission electron microscopy to selectively remove chlorine from suspended metal oxyhalides while observing the transformation at atomic resolution[1]. They produce free-standing CrO and ErO monolayers, demonstrating a synthesis strategy that could potentially be extended to a wider range of layered oxyhalides.

Emerging synthesis routes are expanding the toolbox of two-dimensional metal oxides[2]. The few oxides with layered bulk structures can be exfoliated, whereas non-layered compounds generally require bottom-up growth, interfacial reactions or the removal of a sacrificial component. For example, sacrificial-layer release has produced one-unit-cell-thick free-standing perovskites that contain several atomic planes[3]. Liquid and solid metal–gas interfaces have also expanded the range of accessible ultrathin oxides[4,5]. Each route nevertheless trades chemical scope against crystallinity, substrate coupling, thickness control, transfer fidelity or scalability, while remaining subject to material-specific constraints.

The electron microscope has evolved from an observer into a reactor for materials synthesis. Earlier electron-beam experiments produced nanometre-sized ZnO and CuO monolayers suspended across graphene pores, but their feedstocks, supports and reactions were system specific[6]. In the work of Gao and co-workers, extended crystalline monolayers of related oxyhalides serve directly as precursors for a common conversion strategy. In CrOCl, scanning a 60 keV electron probe drives selective chlorine removal and relaxation of the remaining Cr–O framework into a nearly planar, square-lattice CrO monolayer, forming an atomically sharp lateral interface with unconverted CrOCl (Fig. 1a). Quantitative electron energy-loss spectroscopy establishes an approximately 1:1 Cr:O ratio with no detectable chlorine in the converted regions, while atomic-resolution elemental mapping and electron ptychography resolve both chromium and oxygen sites. Single-crystalline domains exceed 10^4 nm^2, and separate atom-counting analysis indicates an oxygen-vacancy concentration of approximately 0.7%. Spatially selective irradiation also writes a CrO logo and creates arrays of converted regions across multiple suspended windows, with elemental maps confirming chlorine depletion in the patterned regions (Fig. 1b,c).

Why does chlorine leave while oxygen remains? At 60 keV, ab initio molecular dynamics simulations indicate that elastic knock-on collisions alone cannot eject chlorine from free-standing CrOCl. The authors propose that electronic excitation and ionization preferentially weaken Cr–Cl bonds, consistent with density functional theory calculations that show the chlorine-vacancy formation energy to be approximately 2.2 eV lower than that of an oxygen vacancy. Beam chemistry therefore depends on how elastic and inelastic interactions couple to the material's electronic structure[7].

Excess Cr and O segregate into surface CrO_x nanostrips during lattice expansion. Under continued irradiation, time-resolved imaging shows that Cr adatoms redistribute, a nearby nanostrip recedes and the damaged lattice repairs (Fig. 1d), implicating the strips as atomic reservoirs. These reservoirs support repair but also introduce variations in surface coverage, making their control important for producing uniformly bare oxide sheets. Resolving this mechanism could reveal how synthesis and post-synthesis conditioning share the same beam-controlled energy landscape.

The overall footprint of patterning across multiple windows (Fig. 1c) is about $5.3 \times 3.3\ \mu m^2$, although a $1 \times 1\ \mu m^2$ area currently takes roughly 40 min. Previous demonstrations of programmed oxide crystallization[8] and automated defect writing[9] suggest routes towards automated patterning. Yet an ångström-sized probe does not guarantee an equally small chemical footprint. For example, in a reactive carbon–oxygen system, beam tails and inelastic scattering drive etching several nanometres from the probe[10]. Gao and colleagues demonstrate nanoscale chemical lithography and atomically sharp CrOCl–CrO interfaces, although the minimum reproducible feature size remains to be established.

The same dehalogenation logic converts ErOCl into orthorhombic ErO and leaves a coherent ErOCl–ErO boundary. For BiOCl, its monolayer becomes amorphous, whereas a bilayer irradiated at 200 keV retains some chlorine and reconstructs as Bi_4O_4Cl, in which intercalated halogen helps to stabilize the new stacking. These outcomes span *d*-, *f*- and *p*-block metals, but also show that layer number, beam energy and residual halogen can select different products. High-throughput calculations nominate further 1:1 oxide sheets; whether they can be made will depend on suitable oxyhalide precursors and experimentally accessible dose windows[1].

The fabricated phase offers more than structural novelty. Monolayer CrO is an indirect-gap semiconductor with a measured gap of about 2.2 eV and is predicted to support Néel antiferromagnetism below 230 K. In CrO bilayers, experiment and theory identify a strong excitonic feature absent from the monolayer spectrum. Practical translation, however, requires larger crack-free precursors, faster conversion, cleaner transfer and encapsulation. Cracking during the transfer currently limits the available precursor size. Network-like CrO_x nanostrips remain on the converted membranes, limiting surface uniformity. CrO also fragments and becomes amorphous after about 10 min in air, probably through further oxidation. These limitations complicate post-synthesis handling and device integration. Yet as a discovery platform, one instrument initiates a selective reaction, assigns the atomic structure and watches defects evolve. Mapping metals, halogens, layer numbers and beam energies could turn these

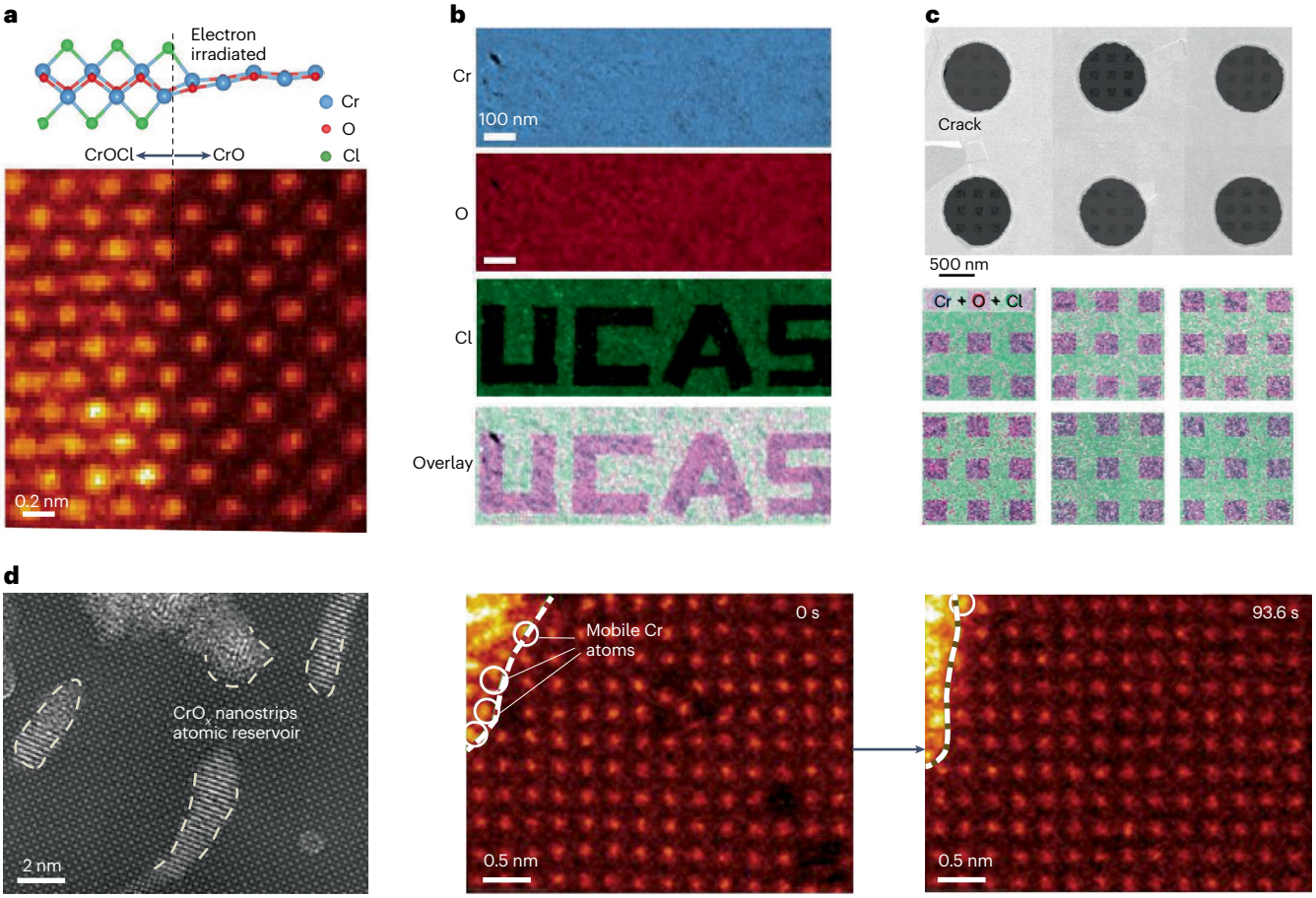


Fig. 1 | Electron-beam conversion, patterning and repair of free-standing chromium oxide. a, Side-view structural model (top) and top-view atomic-resolution scanning transmission electron microscopy (STEM) image (bottom) of a lateral CrOCl–CrO junction. Selective chlorine removal is accompanied by reconstruction of the metal–oxygen framework; the dashed line marks the boundary between the precursor and converted regions. **b**, Spatially controlled conversion of CrOCl. Electron energy-loss spectroscopy elemental maps of Cr, O and Cl together with their overlay reveal the written 'UCAS' logo through chlorine depletion while chromium and oxygen remain. **c**, An overview image shows patterned arrays across six openings in the support film (top), with corresponding composite elemental maps below. A crack is indicated in the overview. **d**, Surface CrO_x nanostrips on the converted membrane (left) and time-resolved atomic-resolution STEM images of lattice repair under continued irradiation (middle and right). Circles identify Cr adatoms, and dashed outlines mark nanostrips or their edges. Between 0 s and 93.6 s, a nearby nanostrip recedes as the damaged lattice repairs, supporting its role as an atomic reservoir. Figure adapted from ref. 1, Springer Nature Limited.

first transformations into predictive rules for oxides inaccessible from layered bulk parents.

Ali Zavabeti
School of Engineering, RMIT University, Melbourne, Victoria, Australia.
e-mail: ali.zavabeti@rmit.edu.au

References

1. Gao, M. et al. *Nat. Mater.* https://doi.org/10.1038/s41563-026-02793-2 (2026).
2. Zhou, K. et al. *Adv. Mater.* **35**, 2207774 (2023).
3. Ji, D. et al. *Nature* **570**, 87–90 (2019).
4. Zavabeti, A. et al. *Science* **358**, 332–335 (2017).
5. Zhang, B. Y. et al. *Nat. Mater.* **20**, 1073–1078 (2021).
6. Ta, H. Q. et al. *Adv. Sci.* **8**, 2100619 (2021).
7. Yoshimura, A. et al. *Nanoscale* **15**, 1053–1067 (2023).
8. Jesse, S. et al. *Small* **11**, 5895–5900 (2015).
9. Klein, J. et al. *Nature* **653**, 715–722 (2026).
10. Noisternig, S. M., Rentenberger, C., Gammer, C., Karnthaler, H. P. & Kotakoski, J. *Ultramicroscopy* **265**, 114019 (2024).

Competing interests

The author declares no competing interests.